



Microwave dielectric properties of B₂O₃-doped ZnTiO₃ ceramics made with sol-gel technique

S.P. Wu*, J.H. Luo, S.X. Cao

College of Chemistry and Chemical Engineering, South China University of Technology, Guangzhou, 510641, China

ARTICLE INFO

Article history:

Received 7 September 2009
Received in revised form 9 April 2010
Accepted 24 April 2010
Available online 21 May 2010

Keywords:

Ceramics
Sol-gel growth
Electronic properties

ABSTRACT

Nano-sized B₂O₃-doped ZnTiO₃ particles were successfully synthesized through sol-gel technique. The crystallization temperature of ZnTiO₃ from sol-gel process was confirmed at 800 °C by the X-ray diffraction (XRD), thermo gravimetric (TG) and differential scanning calorimetry (DSC) analysis. The B₂O₃ content, the high molding pressure and the sintering temperature had great influence on microstructure and the dielectric properties of materials. According to scanning electron microscopy (SEM) analysis, when sintering reagent (B₂O₃) content was 1 wt.%, the grain growth of ZnTiO₃ sintered at 900 °C was anisotropic, and the grain became regular disc structure with a diameter of 2 μm and thickness of 0.3 μm, which might be attributed to the selective growth of crystal grain in a preferential direction. As-prepared 1.0 wt.% B₂O₃-doped ZnTiO₃ sintered at 900 °C for 4 h possessed excellent dielectric properties: $Q \times f = 49,000$ GHz, $\epsilon_r = 8.87$, $\tau_f = -32.35$ ppm/°C. The nano-sized, uniform grains contributed to the high quality factor. The porous bulk ceramics contributed to the low dielectric constant.

© 2010 Elsevier B.V. All rights reserved.

1. Introduction

With the continuous trend of development in wireless communication, considerable researches had focused on microwave ceramics with excellent dielectric behaviors and low sintering temperature. Recent work had demonstrated that ZnTiO₃-based ceramics were a promising material for high performance of microwave devices and more preferably for low-temperature co-fired ceramics (LTCCs) [1,2].

It is well known that the sol-gel process has considerable advantages over conventional solid-state reaction, such as excellent compositional control, lower crystallization temperature and nano-sized precursor powders [3,4]. Many researchers have reported the preparation of ZnTiO₃ powders by sol-gel method [5,6], but their attentions mostly concentrated on the preparation methods and the characterizations of ZnTiO₃ powders. Zhao et al. reported that the crystallization of ZnTiO₃ synthesized by a sol-gel process took place above 500 °C. The formation of ZnTiO₃ was a slow reaction process, which led to the formation of large particles. The size of the ZnTiO₃ particles calcined at 900 °C for 2 h was 30–50 μm [7]. Wang et al. synthesized nanometer scale cubic ZnTiO₃ by sol-gel method at a lower temperature of 600 °C, and found its average crystalline size is 8–10 μm [8]. Chai et al. suggested that the cubic Zn₂Ti₃O₈ varies to hexagonal ZnTiO₃ gradually

from 600 to 800 °C, and the optimal calcination temperature of nano-sized ZnTiO₃ powder was 800 °C. The average grain size of ZnTiO₃ ceramics was 20–50 nm [9]. Hou et al. pointed out the single phase of ZnTiO₃ could only exist in a narrow temperature range. When the temperature increased above 900 °C, the pure ZnTiO₃ would decompose into Zn₂TiO₄ and TiO₂ [10].

In this paper, nano-sized ZnTiO₃ powders were successfully synthesized by sol-gel method. The sintering behavior of nano-sized ZnTiO₃ powders was investigated. The effect of the B₂O₃ content, the molding pressure and temperature on the sintering behavior and the microwave dielectric properties of ZnTiO₃ ceramics were also investigated.

2. Experimental

2.1. Preparation of nano-sized ZnO–TiO₂ particles with sol-gel technology

The ZnTiO₃ particles doped with B₂O₃ were prepared by the following method: zinc acetate and B₂O₃ were dissolved in deionized water as solution A; titanium butoxide (C₁₆H₃₆O₄Ti) was dissolved in ethanol (CH₃CH₂OH) as solution B; ethanol and acetic acid (CH₃COOH) were dissolved in deionized water to obtain solution C. The B₂O₃ was employed as sintering reagent, and its content varied from 0.5 to 4.0 wt.% according to the total weight. The solution B was added drop-wise to solution C under vigorous stirring to form sol. Solution A was dropped to above-mentioned sol to make a transparent solution, which was dried to get gel. The gel was milled into powders, and then processed within electric stove (Nabertherm, LH1320/12, German) at high temperature (600–800 °C) for 3 h to obtain nano-sized particles.

Particles were pressed into pellets with 14 mm in diameter and 6–10 mm in thickness under 40–400 kgf cm⁻² isostatically with a hydrostatic press (Haiou, KSTY70, China). The pellets were sintered at 850–950 °C for 4 h to produce ceramic specimen.

* Corresponding author. Tel.: +86 20 87112897; fax: +86 20 87112897.
E-mail address: chwsp@scut.edu.cn (S.P. Wu).

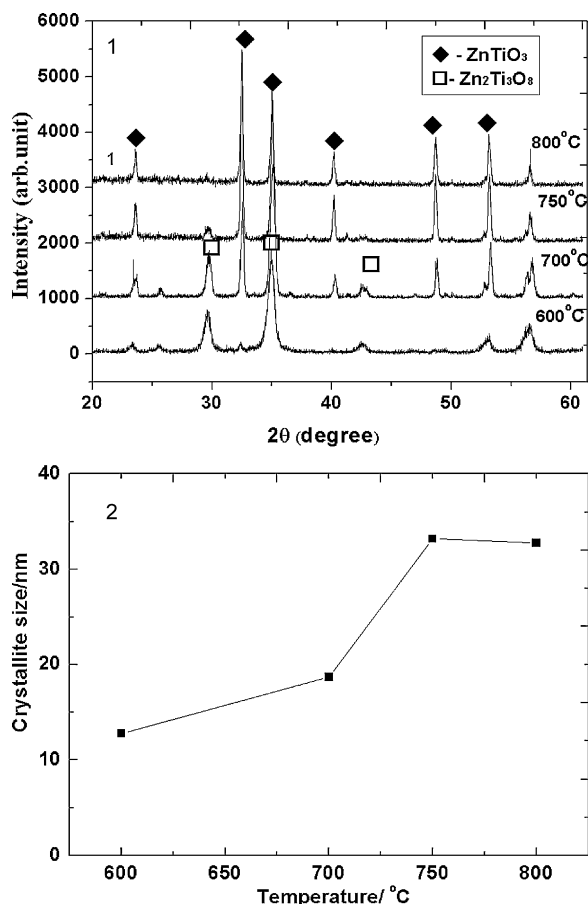


Fig. 1. XRD patterns (1) and grain size (2) of ZnO–TiO₂ particles synthesized by sol–gel technique at different temperatures.

2.2. Characterizations

The powders were analyzed by X-ray diffraction (Rigaku, D/max-III A, Japan) with Cu K α radiation of 2θ from 20 to 70°. Thermo gravimetric (TG) and differential scanning calorimetry (DSC) was carried out with a thermal analyzer (TA, SDT Q600, U.S.A.) in a N₂ flow. The bulk density of ceramics was measured by the Archimedes drainage method. Microstructure observations of the nano-ceramics were performed by scanning electron microscopy (SEM) (Zeiss, LEO 1530 VP, German). Microwave dielectric constants (ϵ_r) and the quality values $Q \times f$ at microwave frequencies were measured by Hakki-Coleman dielectric resonator method using a Network Analyzer (Agilent, E5071B, U.S.A.). Temperature coefficient of resonant frequency (τ_f) was measured by the same method using an Invar cavity in the temperature range from 25 to 75 °C. τ_f was calculated by the following Eq. (1):

$$\tau_f = \frac{f_{75} - f_{25}}{f_{25} \times 50} \quad (1)$$

where f_{75} and f_{25} represent the resonant frequency at 75 and 25 °C, respectively.

3. Results and discussion

3.1. Preparation of nano-sized ZnO–TiO₂ particles

When sintering temperature was 600 °C, the crystal phase of ZnO–TiO₂ particles was identified (in Fig. 1(1)) to be cubic Zn₂Ti₃O₈, which was a low-temperature formation of ZnO–TiO₂ materials as reported by Yamaguchi et al. [11]. A strong peak of hexagonal ZnTiO₃ appeared as the temperature increased to 700 °C. The peak strength of hexagonal ZnTiO₃ increased with an increasing temperature. It indicated that the transformation of Zn₂Ti₃O₈ to ZnTiO₃ occurred. The process finished at 800 °C and pure hexagonal ZnTiO₃ was obtained (as given in curve 1). It was agreeable with that reported by Hou et al. [10].

If the crystals had a lower degree of periodicity, a broader diffraction peak appeared. Peak broadening and shifting can also originate from variations in lattice spacing caused by lattice strain. According to the Scherer's Eq. (2), the crystallite size was calculated.

$$d = 57.3 \times \frac{K\lambda}{\beta \cos \theta} \quad (2)$$

where d is the crystallite size, K is a shape factor (0.9), θ is the diffraction angle and β is the full-width at half-maximum of the peak. As seen from Fig. 1(2), the crystalline size of ZnO–TiO₂ particles was only 13 nm when the specimen was sintered at 600 °C, and it linearly increased to 33 nm at 750 °C. According to thermodynamics, the increasing temperature would result in an increase in crystal size. In addition, the phase transformation from Zn₂Ti₃O₈ to ZnTiO₃ was another possible reason for the change.

3.2. Synthesis of ZnO–TiO₂ ceramics through different routine

By the XRD analysis (in Fig. 2(1)), one could see that the main crystal phase was ZnTiO₃ when the ceramics were obtained (see curves 1 and 2) in the temperature scope of 850–900 °C. Traces of cubic Zn₂Ti₃O₈ occurred in the 850 °C, and its peak intensity strengthened as temperature increased. As exhibited in curves 2 and 3, the decomposing temperature of ZnTiO₃ from sol–gel technology was 850 °C, and the phase transformation of ZnTiO₃ to cubic Zn₂Ti₃O₈ finished at 950 °C.

For comparing with the novel sol–gel technology, we further synthesized ZnTiO₃ ceramics through solid method using ZnO ($d_{50} = 0.3 \mu\text{m}$, determined by Coulter LS230) and ultra-fine TiO₂ ($d_{50} = 0.4 \mu\text{m}$) as raw materials. Experimental procedure was provided in literature [11]. The decomposing temperature of solid-synthesized ZnTiO₃ was 925 °C, as given in curve 5 (Fig. 2(1)). The consistency of grains (see Fig. 2(2)) from sol–gel technique gain clearly the advantage of those from solid method (in Fig. 2(3)) under the same molding pressure (40 kgf cm⁻²). Distinct crystalline plane could be found in Fig. 2(2). Dielectric constant of specimen with sol–gel method sintered at 900 °C were about 10, however, that was 22 for that from solid method. It suggested that the ZnTiO₃ ceramics through sol–gel technology has low dielectric constant, which means short delay time for ceramic substrate and high resonant frequency for microwave component application [12].

The crystallizing temperature of ZnTiO₃ was also investigated according to DSC curves in Fig. 3. An obvious exothermic peak appeared at 800 °C, going with an unvaried weight change as exhibited in TG curve. It might be attributed to the crystallization of ZnTiO₃ made through sol–gel technique. After crystallizing, ZnTiO₃ decomposed gradually when temperature increased, and produced a small quantity of Zn₂Ti₃O₈ at 850 °C as given by XRD. It suggested the crystallization mechanism of ceramics derived from nano-sized particles should be different with that from submicron-sized particles because of the small size effect from nano particles. The crystallization temperature of ZnTiO₃ from sol–gel technique was also confirmed by the XRD analysis in Fig. 1(1). The endothermic peak appeared at 950 °C for ZnO–TiO₂ ceramics. It indicated that the decomposition of ZnTiO₃ occurred.

3.3. SEM analysis

SEM micrographs of ZnTiO₃ ceramics synthesized by sol–gel technique sintered at 900 °C for 4 h were shown in Fig. 4. As seen in Fig. 4(1), the grain size was uniform in 0.5–1.5 μm , and obvious crystallographic plane could be observed when 0.5 wt.% B₂O₃ was employed. When B₂O₃ content up to 1 wt.% (see Fig. 4(2)), the liquid sintering mechanism worked. Under the driving motion of thermal surface tension, the growth of grain acted as the leading role according to high temperature dynamics, resulting in a rapid increase in

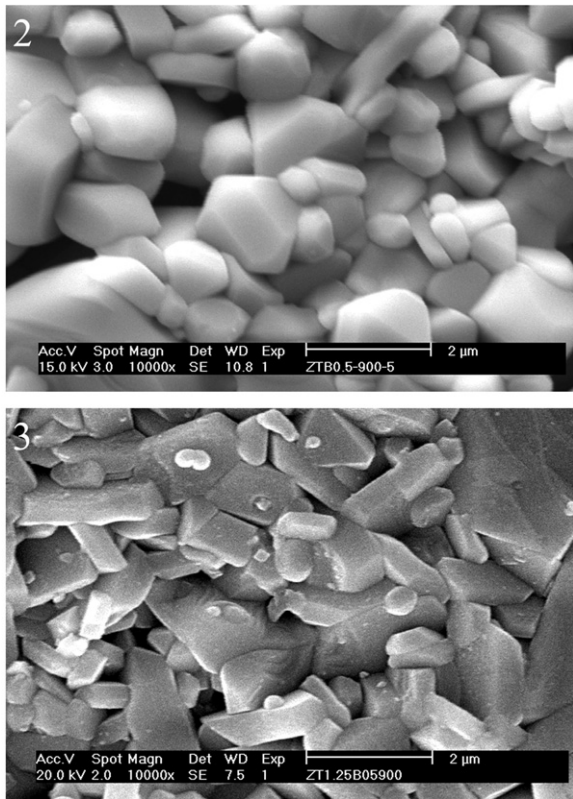
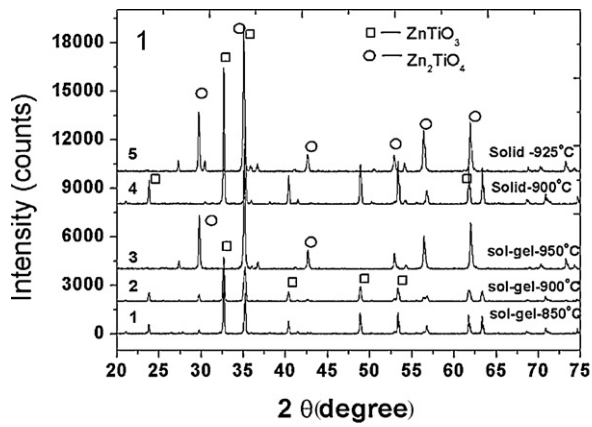


Fig. 2. XRD spectra (1), and SEM micrographs of ZnTiO₃ ceramics through different synthesis routine: (2) sol-gel technique, and (3) solid synthesis method.

grain size. For the polished sample (see Fig. 4(5)), one could observe that as-synthesized ceramics has a porous structure, which might be from the decomposition combustion of organic frame construction. The porous structure would produce an effective influence on dielectric properties. More B₂O₃ content (4 wt.%) should produce an excessive sintering. The grain size increased, uniform grain structure was destroyed, and abnormal grain growth occurred, as was observed in Fig. 4(3).

The molding pressure was another effective factor of microstructure and microwave properties of specimen. From Fig. 4(2), the growth of grain was anisotropic, and the grain became regular disk with a diameter of 2 μm and thickness of 0.3 μm. The bulk ceramics was composed of disk grains, which might be attributed to the selective growth of crystal grain in a preferential direction. In addition, the high molding pressure could destroy the soft-aggregation of nano particles and reduce the thermo diffusion distance between particles during necking stage. Those were all favorable for uniform growth of grain. The

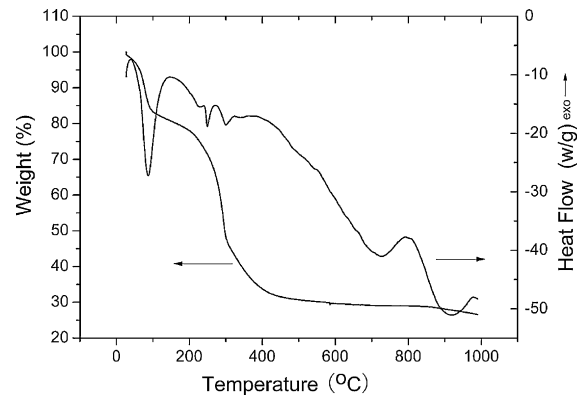


Fig. 3. Thermal analysis of ZnTiO₃ synthesized through sol-gel technique.

nano-sized, uniform, oriented crystal grain produced lower grain defects and grain boundary distortion, which further contributed to the high quality factor ($Q \times f = 49,000$ GHz). It was a reasonable speculation that one could synthesize more excellent disk grains using the dry-press process if more effective hydrodynamic pressure was employed, and ideal dielectric properties of microwave ceramics could be expected.

When specimen was carried out under low-pressure of 40 kgfcm⁻², it was obvious that two kinds of isotropical grain appeared in Fig. 4(4). The larger grains with irregular shape and distort grain boundary could be ascribed to the abnormal diffusion of crystal boundary during sintering. However, the small grain with a size of 500 nm could be considered as the result of local crystallization and growth of particle. Ceramics with so-structure could be called as intergranular nano-ceramics. Nano particles produced strong shrinkage to decrease specific surface energy during sintering. Because the thermo capillary force between particles was not enough to overcome shrinkage among aggregations. The different sintering between inner-aggregation and inter aggregation produced. Densification of inner-aggregation appeared preferentially at sintering because of short interparticle distance. However, with the densification of inner-aggregation developing, the micro gap among grains increased so that the densification of bulk became difficult. It was obvious that a decreasing distance among nanoparticles should inhibit effectively different sintering, reduce porosity factor and promote the densification. The sintering differentiation also produced the abnormal grain. The abnormal grain growth and porous microstructure of specimen contributed to a lower quality factor of 26,000 GHz.

3.4. Microwave dielectric properties

Influences of B₂O₃ content and sintering temperature on quality factor were investigated in Fig. 5(a). As seen in this pattern, quality factors ($Q \times f$) of materials have a similar tendency with sintering temperature. With an increasing temperature, the $Q \times f$ values increased firstly, reached the largest value at 900 °C, and then decreased. In the scope of 850–900 °C, the increase in $Q \times f$ values could be mainly attributed to the promotion of the radial shrinkage ratios. Radial shrinkage ratios of 1 wt.% B₂O₃-doped ZnTiO₃ improved to 15.5% (at 900 °C) from 13% (at 850 °C). The phase transition of ZnTiO₃ contributed to the sharp decrease in $Q \times f$ values of ZnO–TiO₂ ceramics from 900 to 950 °C. The radial shrinkage ratios of specimen were concluded according to Eq. (3):

$$\text{Shrinkage}(\%) = \frac{d_1 - d_2}{d_1} \times 100 \quad (3)$$

where d_1 (d_2) is the diameter of specimen before (after) be sintered respectively.

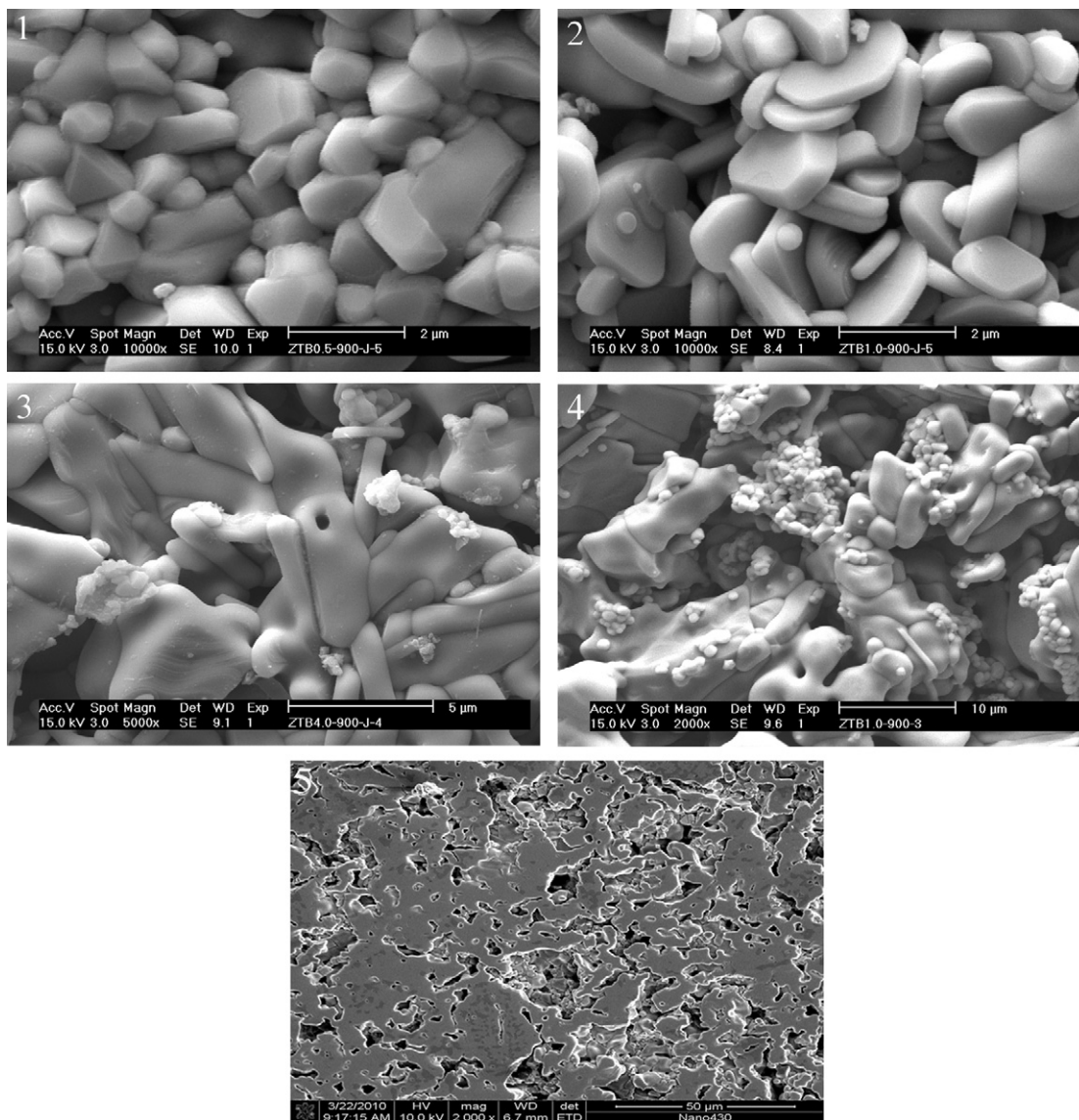


Fig. 4. SEM micrographs of ZnTiO₃ ceramics with different B₂O₃ content sintered at 900 °C: (1) 0.5 wt.%, (2) 1.0 wt.%, and (3) 4.0 wt.% modeled under 400 kgf cm⁻² pressure; (4) 1.0 wt.% under 40 kgf cm⁻² pressure; (5) sample of (2) polished on fracture.

Effects of B₂O₃ content on $Q \times f$ values were analyzed as follows: The $Q \times f$ values of ZnO–TiO₂ ceramics containing a low B₂O₃ content (0.5 wt.%) decreased because of the insufficient liquid sintering, however, high B₂O₃ content (2–4 wt.%) should produce more glass phase. Too much glass should lead to two results: first, dilute the main crystal phase; second, cause abnormal crystalline growth and crystal distortion, as shown in Fig. 4(3 and 4). Both of them could deteriorate quality factor, therefore, appropriate content of B₂O₃ was very important for high quality factor.

The 1.0 wt.% B₂O₃-doped sample sintered at 900 °C got the highest $Q \times f$ value (49,000 GHz), which was higher than that of pure ZnTiO₃ ceramics (19,400 GHz) synthesized through solid-state reaction [13]. In our preliminary work, ZnTiO₃ with 1.0 wt.% B₂O₃ addition sintered at 900 °C for 4 h through solid-state reaction possessed microwave dielectric properties: $\epsilon_r = 22$, $Q \times f = 39,700$ GHz, and $\tau_f = -80$ ppm/°C. It indicated that the sol-gel process had considerable advantages over conventional solid-state reaction.

Microwave dielectric loss could be ascribed to two fields: the intrinsic loss and extrinsic loss. The intrinsic loss was mainly caused by lattice variation modes while the extrinsic loss was mainly dominated by secondary phase, oxygen vacancies, grains sizes and

densification. In this work, the nano-sized, uniform crystal grain could produce a low intrinsic loss, that is to say high quality factor.

When sintering temperature varied from 850 to 900 °C, temperature coefficient of resonant frequency (τ_f) of ZnO–TiO₂ ceramics containing 0.5–2 wt.% B₂O₃ through sol-gel method were stable in -30 – 40 ppm/°C (see Fig. 5(b)) because of the uniform phase. However, the τ_f value of the specimen containing 4 wt.% B₂O₃ improved to 7 ppm/°C, which was ascribed to reaction between B₂O₃ with ZnO to form second glass phase of Zn₃B₂O₆ [6]. The reaction led to a small quantity of dissociative TiO₂, which has a high τ_f value (400 ppm/°C). When the sintering temperature further improved, the phase transform of ZnTiO₃ occurred, producing many TiO₂. TiO₂ contributed to the increasing dielectric constant and τ_f value as given in Fig. 5(b).

As shown in Fig. 5(c), the ϵ_r values of 1.0 wt.% B₂O₃-doped ZnTiO₃ ceramics lowered to 10 (at 850 °C) and 13 (at 950 °C), which were lower than that of ZnTiO₃ ceramics synthesized through solid-state reaction [13,14]. Chaouchi et al. reported that the ϵ_r value of ZnTiO₃ ceramics sintered at 900 °C was 21 with 5.0 wt.% ZnO–SiO₂–B₂O₃ addition [15], however, it was 25 when ceramics was sintered at 950 °C with 15.0 mol.% ZnO–SiO₂–B₂O₃ addition

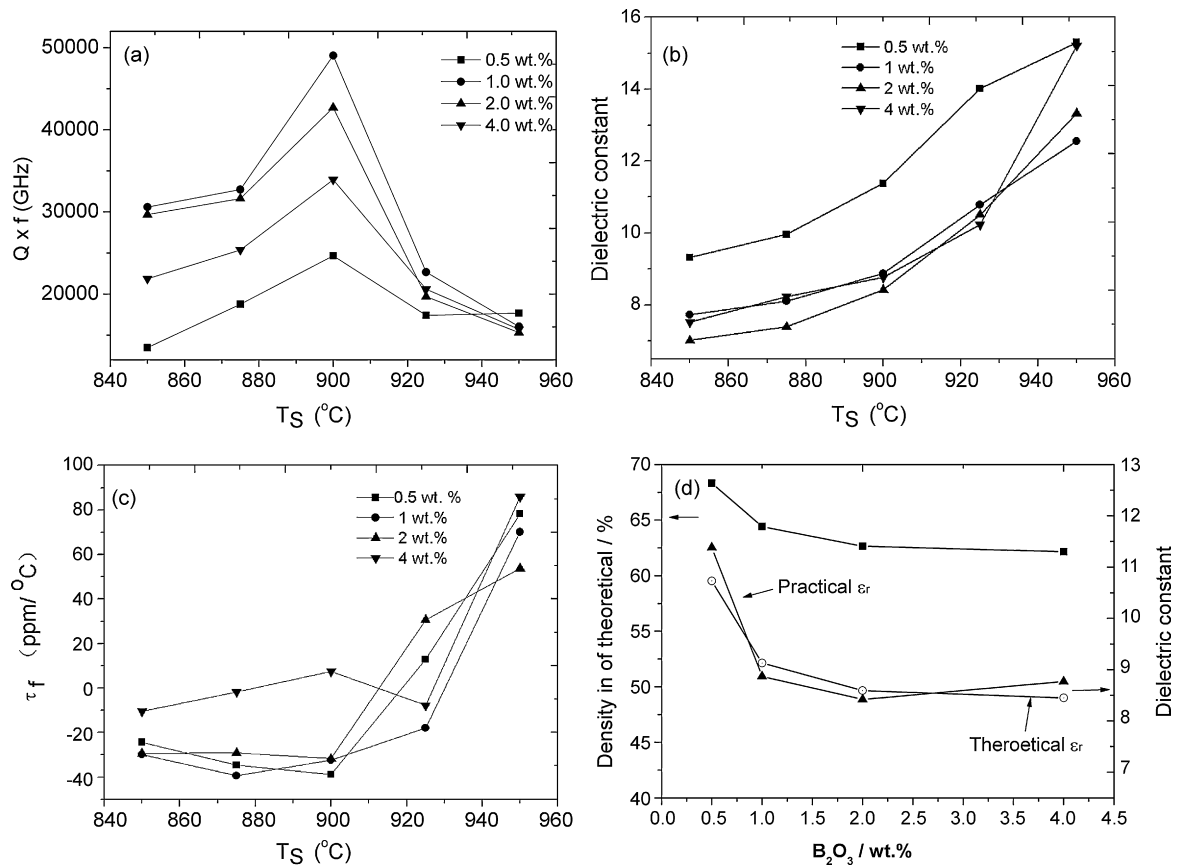


Fig. 5. Microwave dielectric properties of ZnTiO₃ ceramics with different content of B₂O₃ and temperature: (a) $Q \times f$; (b) ϵ_r ; (c) Temperature coefficient of resonant frequency and relation between relative theoretical density and calculated ϵ_r values of ZnTiO₃ (d).

[16]. In this research, dielectric constant linearly decreased as the sintering temperature decreased, regardless of the B₂O₃ content. The main reason for the low dielectric constant was the low ceramic densification. The large shrinking percentage from the nano-sized particles produced many porosities, which led to the low bulk density. One could see from Fig. 5(d), the bulk density of nano-ZnTiO₃ was about 68% of theoretical density (TD = 5.16 g cm⁻³ [17]) by the Archimedes drainage method. The nano-ZnTiO₃ ceramics could be considered as a composite porous ceramics composed of ceramic materials and air ($\epsilon_r = 1$). According to the so-called addition theory, the rule links the resulting dielectric constant (ϵ_r) of a composite versus the ϵ_r of the compounds belonging to the material and characterized by their volume fractions (respectively ϵ_{r1} , γ_1 , and ϵ_{r2} , γ_2):

$$\ln \epsilon_r = \gamma_1 \ln \epsilon_{r1} + \gamma_2 \ln \epsilon_{r2} \quad (4)$$

The preliminary studies indicated that ZnTiO₃ ceramics with 1.0 wt.% B₂O₃ addition sintered at 900 °C for 4 h through solid-state reaction has a bulk density of 4.6 g cm⁻³ (90% of theoretical density) and $\epsilon_r = 22$. According to Eq. (4), the theoretical ϵ_{r1} value of ZnTiO₃ ceramics sintered at 900 °C was 31. Therefore, we could estimate the theoretical ϵ_r values of ZnTiO₃ through sol-gel process, as given in Fig. 5(d). From the pattern, in view of reasonable error, the calculated dielectric constants were very close to test data.

4. Conclusion

In conclusion, nano-sized 0.5–4.0 Wt.% B₂O₃-doped ZnO–TiO₂ particles had been successfully synthesized through sol-gel technique. The crystallization temperature of ZnTiO₃ from sol-gel technique was confirmed at 800 °C by the XRD and thermal anal-

ysis. The crystalline size of ZnO–TiO₂ particles increased as the sintering temperature improved. Microstructure of 1.0 wt.% B₂O₃-doped ZnTiO₃ molded under 400 kgf cm⁻² was regular disk with a diameter of 2 μ m and thickness of 0.3 μ m. ZnTiO₃ ceramics sintered at 900 °C for 4 h possessed excellent dielectric properties: $Q \times f = 49,000$ GHz, $\epsilon_r = 8.87$, $\tau_f = -32.35$ ppm/°C. The nano-sized, uniform, oriented crystal grain produced lower grain defects and grain boundary distortion, which further contributed to the high quality factor. The porous structure of ZnTiO₃ ceramics contributed to a low dielectric constant.

Acknowledgements

This work was supported by the Guangdong-Hong Kong Technology Cooperation Funding Scheme (TCFS) under grant 2008A092000007, The Guangdong Science and Technology projects under grant 2009A080204005 and The Guangdong university-industry cooperation projects under grant 2009B090600075.

References

- [1] H.T. Kim, J.D. Bym, Y. Kim, Mater. Res. Bull. 33 (1998) 963–973.
- [2] H.T. Kim, Y. Kim, M. Valant, D. Suvorov, J. Am. Ceram. Soc. 84 (2001) 1081–1086.
- [3] X.H. Zeng, Y.Y. Liu, X.Y. Wang, W.C. Yin, L. Wang, H.X. Guo, Mater. Chem. Phys. 77 (2002) 209–214.
- [4] Z. Surowiak, M.F. Kupriyanov, D. Czekaj, J. Eur. Chem. Soc. 21 (2001) 1377–1381.
- [5] L.H. Xu, Fang Liana, J. Yang, J.M.F. Ferreir, Ceram. Int. 28 (2002) 549–552.
- [6] A. Golovchanski, H.T. Kim, Y.H. Kim, J. Korean Phys. Soc. 32 (1998) S1167–1169.
- [7] L.L. Zhao, F.Q. Liu, X.W. Wang, Z.Y. Zhang, J.T. Yan, J. Sol-gel Sci. Technol. 33 (2005) 103–106.
- [8] S.F. Wang, F. Gu, M.K. Lu, C.F. Song, S.W. Liu, D. Xu, D.R. Yuan, Mater. Res. Bull. 38 (2003) 1283–1288.

- [9] Y.L. Chai, Y.S. Chang, G.J. Chen, Y.J. Hsiao, *Mater. Res. Bull.* 48 (2008) 1066–1074.
- [10] L. Hou, Y.D. Hou, M.K. Zhu, J.L. Tang, J.B. Liu, H. Wang, H. Yan, *Mater. Lett.* 59 (2005) 197–200.
- [11] O. Yamaguchi, M. Morimi, H. Kawabata, K. Shimizu, *J. Am. Ceram. Soc.* 70 (1987) C97–98.
- [12] S.P. Wu, J. Ni, J.H. Luo, X.H. Ding, *Mater. Chem. Phys.* 117 (2009) 307–312.
- [13] H.T. Kim, S.H. Kim, J.D. Byun, *J. Am. Ceram. Soc.* 82 (1999) 3043–3048.
- [14] L. Jiao, S.P. Wu, X.H. Ding, J. Ni, *J. Mater. Sci: Mater Electron.* 20 (12) (2009) 1186–1192.
- [15] A. Chaouchi, M. Aliout, S. Marinel, S. d'Astorg, H. Bourahla, *Ceram. Int.* 33 (2007) 245–248.
- [16] A. Chaouchi, S. d'Astorg, S. Marinel, M. Aliout, *Mater. Chem. Phys.* 103 (2007) 106–111.
- [17] M.L. Hsieh, L.S. Chen, S.M. Wang, C.H. Sun, M.H. Weng, M.P. Houg, S.L. Fu, *Jpn. J. Appl. Phys.* 44 (2005) 5045–5048.